Macromolecules

ARTICLE

pubs.acs.org/Macromolecules

Stereoregularity of Poly(lactic acid) and their Model Compounds as studied by NMR and Quantum Chemical Calculations

Koto Suganuma,[†,‡] Ken Horiuchi,[‡] Hironori Matsuda,[‡] H. N. Cheng,[§] Akihiro Aoki,[†] and Tetsuo Asakura*[,†]

[†]Department of Biotechnology, Tokyo University of Agriculture and Technology, Koganei, Tokyo, 184-8588, Japan

[‡]Material Analysis Research Laboratories, Teijin Ltd., Hino, Tokyo, 191-8512, Japan

[§]Agriculture Research Service, Southern Regional Research Center, United States Department of Agriculture, 1100 Robert E. Lee Blvd., New Orleans, Louisiana 70124, United States

ABSTRACT: In order to understand the origin of the tacticity splitting in the NMR spectra of poly(lactic acid), monomer and dimer model compounds were synthesized and their ^{1}H and ^{13}C NMR chemical shifts were observed. Two stable conformations were obtained from Ramachandran map calculated as a function of the internal rotation angles for the monomer model using Gaussian 09 calculations. Four preferred conformations were selected and optimized for each dimer model. The conformations of neighboring residues were energetically interdependent. The ^{1}H and ^{13}C chemical shifts for dimer model compounds were calculated by averaging the occurrence probabilities obtained from the optimized conformational energies and the calculated chemical shift of each conformation. It was confirmed that the solvent effect on the tacticity-dependent relative chemical shifts was small from the NMR experiments of the model compound observed in different solvents, dimethyl sulfoxide, chloroform, and chloroform/carbon tetrachloride (20/80 v/v) mixture. Good agreement between observed and calculated chemical shifts was obtained for the relative chemical shifts of isotactic and syndiotactic ^{1}H and ^{13}C NMR peaks of the dimer model compounds. The observed tacticity splitting of poly(lactic acid) at the diad level was rationalized on the basis of these chemical shift calculations.

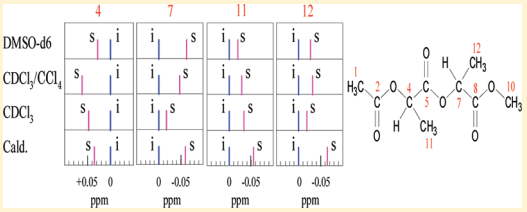

INTRODUCTION

Poly(lactic acid) (PLA) can exist in amorphous and semicrystalline forms in the solid state. In blends of poly(L-lactic acid) (PLLA) and poly(D-lactic acid) (PDLA), the two molecular species can form a 1/1 stereocomplex, and the crystalline structure of the stereocomplex is quite different from that of PLLA or PDLA.[1−5] The stereocomplex PLA has a melting temperature higher than that of the homopolymer by 50 °C. Such a high melting temperature was reported first from a sample isolated from a solution and later from a melt mixture.[2,3] Melt blending of PLLA and PDLA is likely accompanied by the formation of single polymer crystals together with stereocomplex formation, resulting in a mixed crystalline state.[6−8] Yui et al.[9] discovered that a diblock copolymer of PLLA−PDLA could form the stereocomplex easily because of the neighboring effect of the two blocks in the copolymer. On the basis of this result, Fukushima et al.[10] reported that multiblock copolymers of PLLA and PDLA formed the stereocomplex more easily without first forming the single-polymer crystals. However, PLA with short L- and D-block sequences caused lower melting temperature.[11] Thus, it is important to have an improved knowledge of stereoregularity and sequence distribution in PLA samples.

NMR is generally regarded as the best method to study polymer stereoregularity. Many NMR studies have been reported of stereosequence distribution in PLA.[12−18] It is common in the PLA literature to designate the assignments as various combinations of "i" isotactic pairwise relationships (-LL- and -DD-) and "s" syndiotactic pairwise relationships (-LD- and -DL-). In the NMR spectra, the diads -LL- and -DD- are indistinguishable and have the same chemical shifts, but as do the diads -LD- and -DL-. Bero et al.[12] assigned all the CH carbon peaks at the tetrad level and part of the carbonyl peaks at the hexad level, using PLA samples prepared under various reaction conditions and different initiators. Kricheldorf et al.[13] reported the ^{1}H assignments of the CH group of PLA on the basis of the previous ^{13}C assignments with a number of PLA samples prepared under various conditions and using numerous initiators/catalysts. Kasperczyk[14] added more assignments to the previous partial hexad assignments of the carbonyl group of PLA. Partial hexad level assignments of the ^{1}H and ^{13}C peaks of the CH group were reported by Thakur et al.[15] with PLA samples prepared in vials by melt polymerization of various combinations of L-lactide, D-lactide, and *meso*-lactide. Chisholm et al.[17] reported further investigation of the CH ^{1}H and ^{13}C assignments with two-dimensional (2D) NMR such as HETCOR and claimed that previous tetrad level assignments for the CH carbon reported by Kricheldorf et al.[13] were partly in error; This claim was disputed by Kasperczyk[16] and Zell et al.[18] In addition, Zell et al.[18] also reported NMR data from HMQC and HMBC experiments and partly ^{13}C labeled PLA samples and made improved assignments of (sii) and (iis)

Received: August 17, 2011
Revised: October 23, 2011
Published: November 03, 2011

tetrad peaks of the CH proton. Using these several techniques, they reported unambiguous determination of the ^{1}H and ^{13}C tacticity assignment of PLA.[18]

The origin of the tacticity splitting of chemical shifts has been studied for many polymers through semiempirical chemical shift calculation by considering the ^{13}C γ-gauche shielding effect or ^{1}H ring current shielding effect.[19−22] Since the time-averaged occurrence of several conformations of polymer chains in solution must be considered in the chemical shift calculation, it is useful to carry out the conformational energy calculation of model compounds or fragments of the polymer chain. There have been two approaches used, viz., semiempirical energy calculation and quantum chemical calculation. Brant et al.[22] calculated the conformational energy of the PLLA chain using the former method and prepared a rotational isomeric state model of PLLA from the conformational energy maps to reproduce flexible PLA chain and to explain the solution property of the polymer. Meaurio et al.[23] analyzed the carbonyl stretching region of IR spectrum of PLA and discussed the conformational population via simulation of the vibrational behavior of the polymer chain.

The quantum chemical calculations are potentially more accurate and are becoming less time-consuming to do because of increasing computer speed and memory size.[24−27] Two conformational analyses of PLA were reported using quantum chemical calculations.[28] The conformational energies of PLA oligomers were calculated using a quantum chemical method by McAliley et al.,[29] *in vacuo* or in the electronic environment within the condensed phase. Wu et al.[26] determined the equilibrium geometries, IR, total energies and NMR chemical shifts of several lactides, including L-lactide, D-lactide, and three *meso*-lactides. It may be noted that lactides have a ring structure and are different from the structure of polymeric PLA.

In this work, in order to understand the origin of the tacticity splitting in the NMR spectra of PLA, we synthesized the monomer model compound and isotactic and syndiotactic dimer model compounds of PLA and compared the observed and the calculated ^{1}H and ^{13}C NMR chemical shifts of all ^{1}H and ^{13}C nuclei in the models. For comparison, the solvent effect on the tacticity-dependent relative chemical shifts was examined for the dimer model compounds. For the chemical shift calculation, the conformational energy calculation was performed for each isotactic and syndiotactic dimer model compound on the basis of the combination of two energetically stable conformations obtained for the monomer model compound by quantum chemical calculations. The ^{1}H and ^{13}C chemical shifts of all the ^{1}H and ^{13}C nuclei were also calculated for each conformation of the model compounds by the quantum chemical method. The chemical shifts were then obtained for all the ^{1}H and ^{13}C nuclei in isotactic and syndiotactic dimer model compounds. On the basis of the calculated and observed dimer data, an attempt was made to rationalize the tacticity splitting of the CH region of the PLA spectra at the diad level.

EXPERIMENTAL SECTION

Synthesis of Monomer Model Compound (1) of Poly(lactic acid). The monomer model compound (**1**) shown in Figure 1 was synthesized as follows.

Pyridine (523.6 μL) and acetyl chloride (471 mg, 6.0 mmol) were added to a solution of methyl *S*-(−)-lactate (521 mg, 5.0 mmol) in toluene (2.6 mL). The mixture was stirred at room temperature for 2 h.

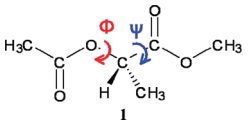

Figure 1. Monomer model compound (**1**) of poly(lactic acid).

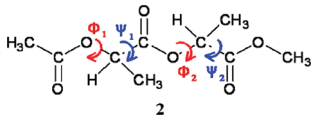

Figure 2. Dimer model compound (**2**) of poly(lactic acid).

Water (2 mL) and tetrahydrofuran (THF) (5 mL) were added to the mixture. The mixture was thoroughly mixed and transferred to a separatory funnel. The two layers (aqueous and toluene) were allowed to separate, and the aqueous layer was discarded. The toluene layer was washed with aqueous sodium hydrogen carbonate solution and passed through a bed of sodium sulfate to remove any residual water. The toluene was evaporated using a rotary evaporator at 40 °C. The product was purified by size exclusion chromatography.

Synthesis of Dimer Model Compound (2) of Poly(lactic acid). The dimer model compound (**2**) shown in Figure 2 was synthesized as follows.

Thionyl chloride ($SOCl_2$) (238 mg, 2 mmol) and DMF (15.5 μL) were added to a solution of (-)-O-acetyl-L-lactic acid (132 mg, 1.0 mmol) in toluene (660.6 μL). The mixture was stirred at 80 °C for 1 h, and the mixture was evaporated using a rotary evaporator at 40 °C. The solution of methyl *S*-(−)-lactate (83 mg, 1.0 mmol) or methyl *R*-(−)-lactate (83 mg, 1.0 mmol) in toluene (660.6 μL) and pyridine (161.1 μL) was added to the mixture. The mixture was stirred at room temperature for 2 h. Aqueous sodium hydrogen carbonate solution (2 mL) and tetrahydrofuran (THF) (5 mL) were added to the mixture. The mixture was thoroughly mixed and transferred to a separatory funnel. The two layers (aqueous and toluene) were allowed to separate, and the aqueous layer was discarded. The toluene layer was washed with aqueous sodium hydrogen carbonate solution and passed though a bed of sodium sulfate to remove any residual water. The toluene was evaporated using a rotary evaporator at 40 °C. The product was purified by size exclusion chromatography.

Preparation of Poly(lactic acid). Copolymer of poly(L-lactic acid) (PLLA) and poly(D-lactic acid) (PDLA), at 50/50 mol %, was prepared by transesterification between PLLA and PDLA. Heat treatment of the blend of PLLA and PDLA with sodium benzoate (1 wt %) was performed on a TG-DTA Instruments (Rigaku Thermo Plus TG 8120) under dry nitrogen atmosphere. A sample was heated from room temperature to 220 °C with a heating rate of 20 K min^{-1}, heated to 250 °C with a rate of 10 K min^{-1}, maintained at 250 °C for 60 min, and quenched into liquid nitrogen. The product was washed with methanol.

NMR Measurement. The ^{1}H and ^{13}C NMR spectra were obtained on a JEOL α-600 spectrometer operating at 600 and 150 MHz, respectively, at room temperature. Deuterated chloroform ($CDCl_3$), deuterated chloroform/carbon tetrachloride (20/80 in vol %) mixture ($CDCl_3/CCl_4$) and deuterared dimethyl sulfoxide (DMSO-d_6) were used as the solvents and the sample concentration was 10% (w/v). Tetramethylsilane (TMS) was used as an internal standard chemical shift reference. The ^{1}H NMR spectra were obtained with a digital resolution of 0.36 Hz/point with 32 K data points together with 45° flip angle and 4s pulse delay. The ^{13}C NMR spectra were obtained with a digital resolution of 1.24 Hz/point with 32 K data points together with 45° flip angle and 2 s pulse delay.

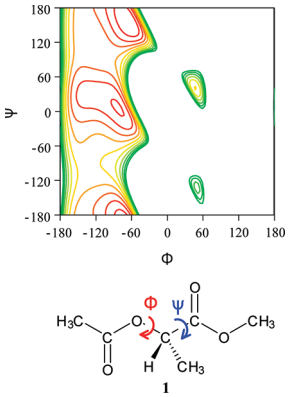

Figure 3. Ramachandran map of the conformational energies as a function of the internal rotation angles, Φ and Ψ for molecule **1**.

Conformational Energy Calculation. The conformational energy calculations of monomer model compound (**1**) were carried out with Gaussian 09 software as a function of the internal rotation angle. The basis set was TZVP.[30−32] The conformational energy calculations were also performed for isotactic and syndiotactic dimer model compounds for the preferred conformations selected from the Ramachandran map of the monomer model compound.

Chemical Shift Calculation. The magnetic shielding tensor was calculated quantum-chemically according to the GIAO method[33−37] for ^{1}H and ^{13}C nuclei of the two preferred conformations of the monomer model compound (**1**). The isotropic chemical shifts were obtained for comparison with the observed chemical shifts. The ^{1}H and ^{13}C chemical shifts of TMS were calculated with the same method. As for the ^{1}H and ^{13}C chemical shift calculations for dimer model compounds, a two-step procedure was used. In each model compound, the relative occurrence probabilities of the preferred conformations were first calculated by Boltzmann distribution on the basis of the difference in the conformational energy. Since the chemical shifts were calculated for each conformation quantum-chemically, the chemical shift of each configuration could be obtained by taking into account both the relative occurrence probability and the chemical shifts of each conformation.

■ RESULTS AND DISCUSSION

(1). Ramachandran Map of Monomer Model Compound (1) as a Function of the Internal Rotation Angles, Φ and Ψ The conformational energies of monomer model compound, **1**, were calculated with Gaussian 09 as a function of the internal rotation angles, Φ and Ψ, and plotted as shown in Figure 3.

According to our calculations, there are two energetically stable states at (Φ,Ψ) values of (−66°, 155°) and (−82°, 7°). Earlier, McAliley et al.[29] calculated the conformational energies of PLA trimer model as a function of the internal rotation angles, Φ and Ψ, by a quantum chemical method (electron density functional theory at the B3LYP/6-31G** level) both *in vacuo* and with a self-consistent reaction field method. Although the model and the details of the quantum chemical methods are different between McAliley et al. and this work, similar Ramachandran maps are obtained. In contrast, the conformational energy map reported by Brant et al.[22] was slightly different. In their map, there were four energetically stable states. The most stable state was the (Φ,Ψ) value of (−73°, 160°), which was similar to the value obtained in this work (Φ,Ψ) = (−66°, 155°). The next energetically stable state was (Φ,Ψ) = (−73°, −48°), which was similar to the value obtained in this work (Φ,Ψ) = (−82°, 7°) although the deviation in Ψ value was slightly larger. There were additional minima at (−160°, 160°) and (−160°, −48°) in their model which was not predicted in our calculations. However, the fractions of the conformations in the map reported by Brant et al. were 55% for (Φ,Ψ) = (−73°, 160°), 37% for (Φ,Ψ) = (−73°, −48°), and sum of other two conformations was 8% at room temperature. In our case, the fraction of the conformations is 74% for (Φ,Ψ) = (−66°, 155°) and 26% for (Φ,Ψ) = (−82°, 7°) at room temperature. Thus, the difference in the maps between the results by Brant et al. and this work is relatively small although the method of calculations seems quite different. The two energetically stable states at (Φ,Ψ) values of (−66°, 155°) and (−82°, 7°) are shown in Figure 4 as ball-and-stick models.

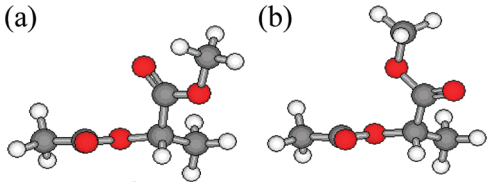

Figure 4. Ball-and-stick models of two energetically preferred conformations of monomer model compound (**1**). (a) The most stable conformation, (Φ,Ψ) = (−66°, 155°). (b) The second stable conformation, (Φ,Ψ) = (−82°, 7°).

Table 1. ^{1}H (Upper) and ^{13}C (Lower) Chemical Shifts (ppm) from TMS of the Monomer Model Compound (1) together with the Energy Difference (Δ*E*) and Probability (%)

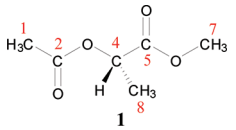

		calcd			
		conformation a	conformation b	average	obsd
Δ*E* (kJ/mol)		0.00	2.66		
probability (%)		74.3	25.7		
^{1}H	1	2.00	1.96	2.00	2.12
	4	4.88	4.84	4.87	5.08
	7	3.61	3.56	3.60	3.74
	8	1.37	1.39	1.38	1.48
^{13}C	1	20.82	20.93	20.84	20.31
	2	177.50	177.48	177.50	170.00
	4	72.59	74.35	72.67	68.25
	5	180.05	179.78	179.98	171.00
	7	53.62	53.78	53.66	51.97
	8	17.95	18.53	18.01	20.31

Although the position of oxygen atom changes almost in the opposite direction in the molecules due to the difference in the internal rotation angle of Ψ, the basic arrangements of the inner backbone atoms are about the same.

(2). ^{1}H and ^{13}C Chemical Shift Calculations of Monomer Model Compound (1). The ^{1}H and ^{13}C chemical shifts were calculated with the quantum chemical method for all ^{1}H and ^{13}C nuclei of the monomer model compound (**1**) with only two conformations, (a) (Φ,Ψ) = (−66°, 155°), and (b) (−82°, 7°). The calculated ^{1}H and ^{13}C chemical shifts (ppm) are listed in

dx.doi.org/10.1021/ma2018777 |*Macromolecules* 2011, 44, 9247–9253

Table 1 together with the energy difference (ΔE, in kJ/mol), and probability (%).

The observed ^{1}H and ^{13}C NMR chemical shifts of the monomer model (**1**) (also listed in Table 1) were obtained in deuterated chloroform. Spectral assignments were carried out with the usual NMR procedures. The calculated chemical shifts are plotted against the observed ones in Figure 5.

High correlation coefficients are obtained, viz., 0.9996 (^{1}H NMR) and 0.9999 (^{13}C NMR).

(3). Conformational Energy Calculations of the Dimer Model (2). The conformational energies of the four conformations for each isotactic and syndiotactic dimer model compound (**2**) were calculated by the quantum chemical method. The combinations of energetically stable states of two preferred conformations selected from monomer model (**1**) were the initial four conformations of the dimer model (**2**). The D-isomer of syndiotactic dimer model was derived by flipping the sign of the Z coordinate of the $X-Y-Z$ coordinate. The initial (Φ,Ψ) and the final (Φ,Ψ) values after optimization by quantum chemical calculations are summarized in Table 2. The conformational energies of the final conformations are also listed in Table 3.

It is noted that there are significant differences between the products of the *monomer* model compound conformational probabilities and the final *dimer* model compound conformational probabilities, even though the conformation of each dimer residue is similar to those derived for the monomer model compounds. Specifically, for isotactic dimer model compound, the products of the monomer model compound conformational probabilities were 0.55, 0.19, 0.19, and 0.07 for L1L1, L1L2, L2L1, and L2L2, respectively, but 0.77, 0.18, 0.03, and 0.02, respectively, for the final dimer model compound conformational probabilities. Similar (and larger) differences are seen for the syndiotactic dimer model compound. The products of the monomer model compound conformational probabilities were 0.55, 0.19, 0.19, and 0.07 for L1D1, L1D2, L2D1, and L2D2, respectively, but 0.13, 0.31, 0.45, and 0.11, respectively, for the final dimer model compound conformational probabilities. The larger differences in the syndiotactic case are probably due to the energetics of the different asymmetric carbon atoms in the syndiotactic dimer model compounds. In any case, the conformations of neighboring PLA residues are energetically interdependent.

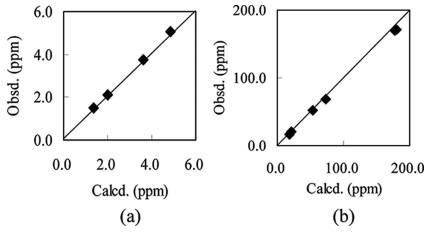

Figure 5. Comparison of the calculated and observed chemical shifts of (a) ^{1}H and (b) ^{13}C nuclei of monomer model compound (**1**) of poly(lactic acid).

(4). ^{1}H and ^{13}C Chemical Shift Calculations of Dimer Model (2) and Comparison between the Calculated and Observed Chemical Shifts. The ^{1}H and ^{13}C chemical shifts of each conformation of the dimer model (**2**) were calculated. The ^{1}H and ^{13}C chemical shifts (ppm) of all ^{1}H and ^{13}C nuclei except for two terminal CH_3 groups are listed in Table 3 together with the energy difference (ΔE, in kJ/mol) and the conformational probabilities (%). The observed chemical shifts were obtained through ^{1}H and ^{13}C NMR analysis of the dimer model in DMSO-d_6, $CDCl_3$/CCl_4 (20/80 in vol %) mixture and $CDCl_3$. The peak assignments were achieved readily with usual NMR procedures as well as comparison with the monomer model compound. The observed ^{1}H and ^{13}C chemical shifts are shown as stick spectra (Figures 6 and 7, respectively). In the literature, the NMR solvent of PLA was usually $CDCl_3$, but DMSO-d_6 was used occasionally although the solvent polarity is quite different. CCl_4 is an inert solvent but PLA is insoluble in CCl_4. However, the dimer model compound is soluble in $CDCl_3$/CCl_4 (20/80 in vol %) mixture, where $CDCl_3$ is used also for NMR field locking. Although the characteristics of three solvent systems are quite different, the relative tacticity splitting of the dimer model compounds shows no significant difference among the solvents. This means that the relative tacticity splitting is due to inherent difference between two compounds, and we can compare the observed chemical shifts with the calculated chemical shifts *in vacuo*.

Note that the observed chemical shift differences are very small between isotactic and syndiotactic dimer models for

Table 2. Initial Internal Rotation Angles (Φ_1, Ψ_1, Φ_2, Ψ_2) and Final Ones (Φ_1, Ψ_1, Φ_2, Ψ_2) of the Dimer Model Compound (2) after Optimization by Gaussian 09 Software

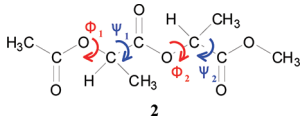

2

		isotactic type for conformation				syndiotactic type for conformation			
		L1L1	L1L2	L2L1	L2L2	L1D1	L1D2	L2D1	L2D2
initial (deg)	Φ_1	−66.0	−66.0	−82.0	−82.0	−66.0	−66.0	−82.0	−82.0
	Ψ_1	155.0	155.0	7.0	7.0	155.0	155.0	7.0	7.0
	Φ_2	−66.0	−82.0	−66.0	−82.0	66.0	82.0	66.0	82.0
	Ψ_2	155.0	7.0	155.0	7.0	−155.0	−7.0	−155.0	−7.0
final (deg)	Φ_1	−69.6	−71.1	−134.5	−81.9	−84.5	−76.1	−70.5	−71.9
	Ψ_1	160.3	162.8	50.4	−10.6	−175.3	173.2	−16.6	−13.8
	Φ_2	−73.9	−74.9	−71.5	−74.9	73.7	72.1	74.1	75.6
	Ψ_2	166.8	−11.4	165.5	−11.0	−162.3	11.6	−166.6	11.2

dx.doi.org/10.1021/ma2018777 |*Macromolecules* 2011, 44, 9247–9253

Table 3. ^{1}H (Upper) and ^{13}C (Lower) Chemical Shifts (ppm) from TMS of the Isotactic and Syndiotactic Dimer Model Compounds (2) together with the Energy Difference (ΔE) and Probability (%) of Each Conformation[a]

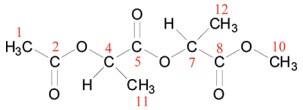

2

		isotactic type for conformation						syndiotactic type for conformation					
		calcd						calcd					
		L1L1	L1L2	L2L1	L2L2	average	obsd	L1D1	L1D2	L2D1	L2D2	average	obsd
ΔE (kJ/mol)		0.00	3.71	8.03	9.04			3.11	0.96	0.00	3.45		
probability (%)		77.3	17.5	3.1	2.1			13.0	30.6	45.1	11.3		
^{1}H	4	4.47	4.51	5.39	4.87	4.48	5.11	4.51	4.78	4.45	4.51	4.52	5.16
	7	4.56	4.60	4.46	4.56	4.57	5.17	4.05	4.54	4.48	4.55	4.51	5.15
	11	1.58	1.53	1.35	1.44	1.56	1.57	1.17	1.46	1.55	1.52	1.50	1.53
	12	1.46	1.48	1.42	1.43	1.46	1.53	1.14	1.45	1.38	1.41	1.39	1.51
^{13}C	4	66.01	65.50	64.33	65.11	65.96	68.30	59.61	64.76	66.92	66.42	66.22	68.44
	7	65.37	66.62	65.78	66.96	65.46	69.00	61.12	67.04	65.35	66.71	66.09	69.14
	11	16.65	16.57	16.42	17.65	16.63	16.68	15.78	16.55	17.14	17.23	17.05	16.77
	12	16.61	17.38	16.53	17.23	16.63	16.75	15.60	17.13	16.42	17.17	16.58	16.80
	2	182.87	182.71	181.45	182.11	182.84	170.33	172.31	182.46	182.96	182.82	182.80	170.14
	5	182.82	182.69	182.53	183.82	182.79	170.24	173.40	182.38	182.79	183.06	182.68	170.08
	8	183.55	183.67	182.83	183.34	183.56	170.65	173.50	183.41	183.11	183.65	183.28	170.44

[a] The observed chemical shifts in $CDCl_3$ are listed here; more chemical shift data are also shown in Figures 6 and 7.

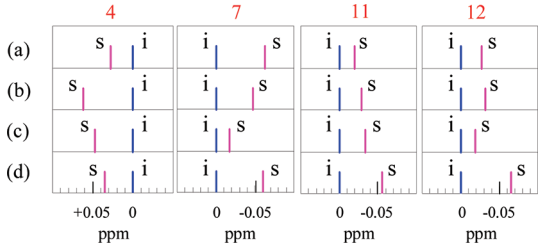

Figure 6. Comparison of the observed and calculated ^{1}H chemical shifts (in ppm) of dimer model compound (**2**) of poly(lactic acid) shown as stick spectra. The solvent is (a) DMSO-d_6, (b) $CDCl_3/CCl_4$ (20/80 in vol %) mixture, and (c) $CDCl_3$. The calculated chemical shifts are shown as (d). The chemical shifts are shown relative to the isotactic chemical shift. The blue stick corresponds to isotactic and the pink syndiotactic.

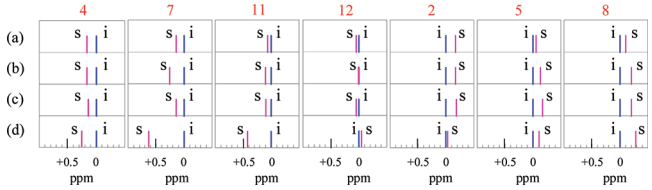

Figure 7. Comparison of the observed and calculated ^{13}C chemical shifts (in ppm) of dimer model compound (**2**) of poly(lactic acid) shown as stick spectra. The solvent is (a) DMSO-d_6, (b) $CDCl_3/CCl_4$ (20/80 in vol %) mixture, and (c) $CDCl_3$. The calculated chemical shifts are shown as part d. The chemical shifts are shown relative to the isotactic chemical shift. The blue stick corresponds to isotactic and the pink syndiotactic.

poly(lactic acid) for both nuclei when compared with the chemical shift difference in other polymers.[13,14] It is instructive to compare the relative peak position for each nucleus between the isotactic and syndiotactic dimer model compounds. As shown in Figure 6, it is interesting that the isotactic and syndiotactic peaks are reversed in their relative peak positions for H-4 and H-7 in the dimer model. Thus, syndiotactic peak resonates downfield for H-4, but upfield for H-7 relative to the isotactic peak. This trend has been reproduced qualitatively by the ^{1}H chemical shift calculations as shown in Figure 6. From Table 3, it can be seen that the calculated syndiotactic chemical shifts are almost the same between the H-4 and H-7, i.e., 4.52 and 4.51 ppm, respectively. However, the isotactic chemical shifts are significantly different between H-4 and H-7, i.e., 4.48 and 4.57 ppm, respectively. Among the four calculated chemical shifts of H-4 of isotactic dimer model, the value for L2L1 is remarkably large; however, its probability is only 3.1% and therefore negligible when all conformations are considered. The chemical shift difference between H-4 and H-7 in L1L1 with the occurrence probability 77.3% seems to be the origin of the reversed peak positions between syndiotactic and isotactic dimer models (Table 3). In contrast, the observed relative peak positions are the same for the two CH_3 protons, H-11 and H-12; i.e., the syndiotactic peak resonates upfield relative to the isotactic peak. This trend has again been reproduced by the chemical shift calculations. As shown in Figure 7, the observed CH carbon peaks, C-4 and C-7, of syndiotactic dimer model compound resonate downfield from the positions of isotactic peaks. Similarly, the observed CH_3 carbon peak, C-11, of syndiotactic dimer resonates downfield from the position of isotactic peak. However, no significant chemical shift difference is observed for the

dx.doi.org/10.1021/ma2018777 |Macromolecules 2011, 44, 9247–9253

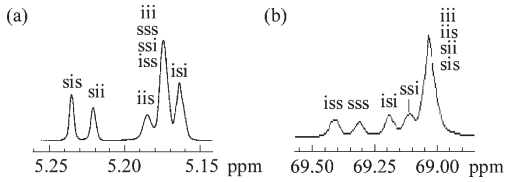

Figure 8. ^{1}H and ^{13}C NMR spectra of copolymer of PLLA and PDLA in $CDCl_3$. (a) Expanded CH proton region in the ^{1}H NMR spectrum.[13] (b) Expanded CH carbon region in the ^{13}C NMR spectrum. The assignments were reported previously.[13,18]

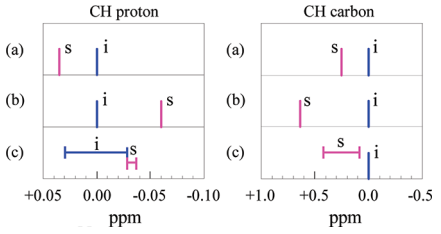

Figure 9. Calculated ^{1}H (left: (a) H-4, (b) H-7) and ^{13}C (right: (a) C-4, (b) C-7) chemical shifts (in ppm) of dimer model compound (**2**) of poly(lactic acid). (c) Observed ^{1}H (left) and ^{13}C (right) diad chemical shifts of poly(lactic acid). All chemical shifts are shown relative to the isotactic chemical shift. The blue stick corresponds to isotactic and the pink syndiotactic.

CH_3 carbon, C-12, between the two samples. As for the three carbonyl carbons, C-2, C-5, and C-8, all syndiotactic peaks in the dimer model compound are found to be upfield from the isotactic peaks. Again, these trends have been reproduced by the chemical shift calculations.

Thus, chemical shift calculations for isotactic and syndiotactic diad model (**2**) of PLA coupled with the conformational energy calculations can be used to predict time-averaged local conformation and tacticity splitting in this PLA dimer. The chemical shift is a good indicator that reflects the local conformations in solution.

(5). Analysis of PLA Stereoregularity at the Diad Level on the Basis of the Chemical Shift Calculations of the Diad Model Compounds. ^{1}H and ^{13}C NMR have been used to analyze the stereoregularity of PLA.[12−18] The tacticity assignments have been reported at the hexad level partly for the carbonyl carbon group, but the assignments of the CH_3 group have not been reported yet. As for the CH group, Figure 8 shows the expanded ^{1}H and ^{13}C peaks of PLA in $CDCl_3$ together with the assignments at the tetrad level reported previously.[13,18]

When the previous assignments of the tetrads in Figure 8 are reduced to the diad level, an interesting trend can be seen. In the ^{1}H spectrum, the isotactic diad-centered tetrad peaks tend to resonate at lower field and the chemical shift range is relatively large compared with the syndiotactic diad-centered tetrad peaks. Contrary to the ^{1}H NMR case, in the ^{13}C NMR spectrum the syndiotactic diad-centered tetrad peaks resonate at lower field and the chemical shift range is relatively large compared with the isotactic diad-centered tetrad peaks. These trends are summarized in Figure 9, together with the calculated and observed CH chemical shifts of the dimer model compounds mentioned above.

The positions of the calculated and the observed chemical shifts are shown relative to the isotactic peak. As noted above, the calculated syndiotactic H-7 appears upfield relative to the isotactic peak, but the opposite trend is found for H-4 in the dimer model compound. In PLA, the stereoregularity of the CH proton was reported to be more sensitive to the lactic acid units attached to the end with the hydroxyl group ("O-terminus").[18] This corresponds to position 7 in the dimer model compound. Thus, the observed ^{1}H chemical shift of PLA should be compared with the calculated chemical shift of H-7, rather than H-4. For the calculated ^{13}C peaks, C-4 and C-7, the syndiotactic peaks appear downfield relative to the isotactic peaks in the dimer model compound. In PLA, the CH carbon was reported to be more sensitive to the lactic acid unit attached to the end with the carboxylic group ("C-terminus"),[18] which corresponds to peak C-4 in the dimer model compound. Thus, the diad level splitting of ^{1}H and ^{13}C NMR spectra of the CH group of PLA can be satisfactorily interpreted by the chemical shift calculation performed here.

The agreement between observed and calculated shifts in PLA means that the time-averaged local conformations predicted in this work are applicable to PLA in solution, and the origin of tacticity splitting in PLA is due to both time-averaged conformations and the chemical shifts of the conformations. At present, it is still unclear why the width of the tacticity splitting of the CH group in PLA is different for ^{1}H and ^{13}C. Further chemical shift calculation at the tetrad level of PLA by taking into account the time-averaged conformations for longer model compounds will hopefully provide more information in the future.

■ ACKNOWLEDGMENT

T.A. acknowledges support from Grant-in-Aid for Scientific Research from Ministry of Education, Science, Culture and Supports of Japan (23245045) and (21550112). The authors would like to thank Mr. Masato Komiyama at Teijin Pharma Ltd. for his support on the synthesis of the model compounds and Dr. Masao Hirasaka at Teijin Ltd. for his support on discussion. Mention of trade names or commercial products in this publication is solely for the purpose of providing specific information and does not imply recommendation or endorsement by the U.S. Department of Agriculture; USDA is an equal opportunity provider and employer.

■ REFERENCES

(1) Okihara, T.; Tsuji, M.; Kawaguchi, A.; Katayama, K. *J. Macromol. Sci. Phys.* **1991**, *B30* (1&2), 119–140.
(2) Ikada, Y.; Jamshidi, K.; Tsuji, H.; Hyon, S.-H. *Macromolecules* **1987**, *20*, 904–906.
(3) Tsuji, H.; Ikada, Y. *Macromolecules* **1993**, *26*, 6918–6926.
(4) Tsuji, H.; Ikada, Y. *Macromolecules* **1992**, *25*, 5719–5723.
(5) Li, L.; Zhong, Z.; de Jeu, W. H.; Dijkstra, P. J.; Feijen, J. *Macromolecules* **2004**, *37*, 8641–8646.
(6) Tsuji, H.; Horii, F.; Nakagawa, M.; Ikada, Y.; Odani, H.; Kitamaru, R. *Macromolecules* **1992**, *25*, 4114–4118.
(7) He, Y.; Xu, Y.; Wei, J.; Fan, Z.; Li, S. *Polymer* **2008**, *49*, 5670–5675.
(8) Tsuji, H.; Ikada, Y. *Macromol. Chem. Phys.* **1996**, *197*, 3483–3499.
(9) Yui, N.; Dijikstra, P. J.; Feijen, J. *Macromol. Chem.* **1990**, *191*, 481–488.
(10) Fukushima, K.; Kimura, Y. *Macromol. Symp.* **2005**, *224*, 133–143.
(11) Fukushima, K.; Furuhashi, Y.; Sogo, K.; Miura, S.; Kimura, Y. *Macromol. Biosci.* **2005**, *5*, 21–29.

(12) Bero, M.; Kasperczyk, J.; Jedlinski, Z. J. *Makromol. Chem.* **1990**, *191*, 2287–2296.
(13) Kricheldorf, H. R.; Boettcher, C.; Tonnes, K. *Polymer* **1992**, *33*, 2817–2824.
(14) Kasperczyk, J. E. *Macromolecules* **1995**, *28*, 3937–3939.
(15) Thakur, K. A. M.; Kean, R. T.; Hall, E. S. *Macromolecules* **1997**, *30*, 2422–2428.
(16) Kasperczyk, J. E. *Polymer* **1999**, *40*, 5455–5458.
(17) Chisholm, M. H.; Iyer, S. S.; McCollum, D. G.; Pagel, M.; Werner-Zwanziger, U. *Macromolecules* **1999**, *32*, 963–973.
(18) Zell, M. T.; Padden, B. E.; Paterick, A. J.; Thakur, K. A. M.; Kean, R. T.; Hillmyer, M. A.; Munson, E. J. *Macromolecules* **2002**, *35*, 7700–7707.
(19) Tonelli, A. E. *NMR Spectroscopy and polymer microstructure*; VCH Publishers: New York, 1989.
(20) Matsuzaki, K.; Uryu, T.; Asakura, T. *NMR spectroscopy and stereoregularity of polymers*; Japan Scientific Societies Press: Tokyo, 1996.
(21) Tonelli, A. E. *Polymers from the Inside Out*; John Wiley & Sons, Inc.: New York, 2001
(22) Brant, D. A.; Tonelli, A. E.; Flory, P. J. *Macromolecules* **1969**, *2*, 228–235.
(23) Meaurio, E.; Zuza, E.; Lopez-Rodriguez, N.; Sarasua, J. R. *J. Phys. Chem. B* **2006**, *110*, 5790–5800.
(24) Carbone, P.; Ragazzi, M.; Tritto, I.; Boggioni, L.; Ferro, D. R. *Macromolecules* **2003**, *36*, 891–899.
(25) Boggioni, L.; Bertini, F.; Zannoni, G.; Tritto, I.; Carbone, P.; Ragazzi, M.; Ferro, D. R. *Macromolecules* **2003**, *36*, 882–890.
(26) Wu, W.; Li, W.; Wang, L.; Zhang, P.; Zhang, J. *THEOCHEM* **2007**, *816*, 13–19.
(27) Kang, Y. K.; Byun, B. J. *J. Phys. Chem. B* **2008**, *112*, 9126–9134.
(28) Inai, Y.; Ogawa, H. *Kobunshi Ronbunshu* **2010**, *67*, 214–223.
(29) McAliley, J. H.; O'Brien, C. P.; Bruce, D. A. *J. Phys. Chem. A* **2008**, *112*, 7244–7249.
(30) Schafer, A.; Horn, H.; Ahlnichs, R. *J. Chem. Phys.* **1992**, *97*, 2571–2577.
(31) Schafer, A.; Huber, C.; Ahlnichs, R. *J. Chem. Phys.* **1994**, *100*, 5829–5835.
(32) Becke, A. D. *J. Chem. Phys.* **1993**, *98*, 5648–5652.
(33) London, F. *J. Phys. Radium.* **1937**, *8*, 397–409.
(34) McWeeny, R. *Phys. Rev.* **1962**, *126*, 1028–1034.
(35) Ditchfield, R. *Mol. Phys.* **1947**, *27*, 789–807.
(36) Wolinski, K.; Hilton, J. F.; Pulay, P. *J. Am. Chem. Soc.* **1990**, *112*, 8251–8260.
(37) Cheeseman, J. R.; Trucks, G. W.; Keith, T. A.; Frisch, M. J. *J. Chem. Phys.* **1996**, *104*, 5497–5509.